JOURNAL OF CATALYSIS 61, 39–47 (1980)

A Study of Ruthenium in Zeolite-Y by X-Ray Photoelectron Spectroscopy

LEE A. PEDERSEN AND JACK H. LUNSFORD

Department of Chemistry, Texas A&M University College Station, Texas 77843

Received March 30, 1979; revised May 29, 1979

Ruthenium-exchanged NaY zeolites were studied with X-ray photoelectron spectroscopy in order to determine changes in the location and state of the Ru after subjecting the samples to both oxidizing and reducing environments. When O_2 was excluded from the system, ruthenium remained inside the zeolite cavities following reduction in H_2 and after the zeolite had catalyzed the methanation reaction. At elevated temperatures, before or after reduction, the presence of O_2 resulted in the formation of RuO_2 on the external surface of the zeolite. The peak intensity of the Ru $3d_{5/2}$ line increased by more than a factor of five when the ruthenium migrated to the surface. Positive binding energy shifts of approximately 1 eV were detected for small clusters (< 10 Å) of reduced ruthenium when compared with larger metal particles within the zoelite or on its external surface.

INTRODUCTION

In a recent paper from this laboratory it has been reported that ruthenium metal in zeolite-Y is active for the conversion of carbon monoxide and hydrogen to methane; however, the turnover numbers for this reaction were not significantly different from those obtained for ruthenium on alumina, with the metal in a similar state of dispersion (*1, 2*). In interpreting the results for the RuY zeolite it was important to determine whether the metal remained within the cavities or whether it migrated to the external surfaces of the zeolite crystallites. The metal particle size, based on deuterium chemisorption and electron microscopy, was <10 Å after reduction of the ruthenium with hydrogen, but the size increased to ca. 15 Å following the methanation reaction. Even in the latter case most of the particles were sufficiently small to have remained in the large cavities of the zeolite, but there was no direct evidence to support this location.

The present study was undertaken primarily to determine the location of the metal in the zeolite, and to investigate the conditions under which the ruthenium would migrate to external surfaces. Such migration may be detected by X-ray photoelectron spectroscopy (XPS) since this near-surface technique has a nominal sampling depth of 40 Å, due to the escape depth of the excited electrons. As the metal moves closer to the external surface of the 1 μm zeolite crystallites, more of the ejected electrons are detected. Thus the peak intensity of small metal particles on the surface of the zeolite is greatly enhanced compared to the intensity of the metal within the internal regions of the zeolite.

Minachev *et al.* (*3, 4*) have employed XPS to show that Ag, Pd, and Ni diffuse to the external surfaces of zeolites. By less direct means it has been established that about 50% of the Cu in a Y-type zeolite also migrates to the external surface upon reduction in hydrogen (*5*). Copper in the form of 300-Å crystallites could not be reversibly oxidized to the exchanged cation, but the metal within the zeolites formed Cu^{2+} ions in the exchange sites. The mobility of ruthenium in zeolites under oxidizing versus reducing conditions is particularly interesting. It is well known that the metal forms volatile oxides (*6*) and a recent study has concluded that sintering of supported Ru in oxygen is due to the transport of the metal oxide species (*7*). In contrast the

0021-9517/80/010039-09$02.00/0
Copyright © 1980 by Academic Press, Inc.
All right of reproduction in any form reserved.

same study shows that Ru is less susceptible than Pt to sintering in hydrogen atmosphere.

Changes in oxidation state of the metal ion and the extent of metal–support interactions in a zeolite may also be explored by XPS through the determination of shifts in binding energies. Although an interpretation of binding energy shifts is complicated by other effects, it is evident from this study that small ruthenium clusters (<10 Å) behave differently than somewhat larger metal particles (ca. 15 Å).

EXPERIMENTAL METHODS

Zeolites of 0.5 and 2.0% by weight Ru were prepared from Ru $(NH_3)_6Br_3$ according to the procedure reported previously (*1*). These loadings correspond to 4.5 and 18% of the cation-exchange capacity of the zeolite. One sample of 1% Ru on NaY zeolite was prepared by an incipient wetness technique, using a solution of ruthenium hydroxide and HCl (*8*). The crystallinity of the zeolites before and after pretreatment was checked by means of powder X-ray diffraction, and in all cases a high degree of crystallinity was maintained.

Matheson UHP He (99.995%), H_2 (99.999%), and N_2 (99.999%) were used as received. A mixture of CO and H_2 prepared by Air products was passed through an activated charcoal trap at room temperature to remove carbonyls. Mixtures of 0.02, 0.6, 1.2, 2.2, 11, and 21% dry oxygen in helium were prepared in the laboratory and the oxygen content was verified with a mass spectrometer. Commercial dry air was utilized for air pretreatments.

The photoelectron spectra were obtained with a Hewlett Packard Model 5950A spectrometer using monochromatic Al K_α X-rays (1486.6 eV) and a window width of 20 eV. Pressure in the analyzer chamber during any run was less than 6×10^{-9} Torr. Binding energies were referenced to the Au $4f_{7/2}$ (84.0 eV) line of a gold spot which had been evaporated onto several samples before pretreatment. The Si 2s (154.0) and O 1s (532.3) lines of the zeolite were usually employed as secondary, internal standards for obtaining binding energies of ruthenium and other elements. Using the photoelectron spectrometer in this laboratory several different operators have observed Si 2s binding energies of 154.0 ± 0.2 eV on such diverse materials as NaY zeolite, amorphous silica–alumina, and silica gel. As a reference C 1s was found to be unsuitable when Ru was present.

Charge compensation was achieved by flooding the sample with nearly zero kinetic energy electrons. Binding energies were reproducible to ±0.3 eV or less depending on the broadness of the peak. Because of evidence for reduction of Ni in a NiNaX zeolite by the X-ray beam itself (*9*), spectra were recorded as a function of time. There was no evidence for photoreduction in the zeolites treated at 300°C or higher. All spectra were taken with the sample at ca. 25°C.

For most samples regions of the spectrum corresponding to Si 2p (102.7 ± 0.1), Al 2p (74.7 ± 0.1), and Na 2s (64.3 ± 0.2) of the zeolite were scanned along with the appropriate peak of the transition metal component and the internal standards. Area ratios were obtained using a Dupont Model 310 curve resolver, assuming Gaussian peak shapes. The latter gave a reasonably good fit to the experimental spectra. The areas were corrected using cross sections reported by Scofield (*10*). All peak intensities were normalized to a 1-hr scan.

To facilitate comparison of spectra from different days, concentration ratios of the significant components were calculated. The equation for the intensity of an XPS peak is given by

$$I \propto n\sigma\lambda F K_{sp} \tag{1}$$

where n is the atomic concentration of the element, σ is the cross section for photoelectron emission from the level, λ is the escape depth, and F and K_{sp} are the X-ray flux and a spectrometer detection efficiency, respectively. According to Wagner

(*11*), ratios of λ for different nontransition elements vary by less than 10% provided the kinetic energies of the ejected electrons differ by no more than a factor of two. In this study values of λ were assumed to be the same for all elements. The parameters F and K_{sp} can be combined into a spectrometer constant so that one may obtain the concentration ratio

$$\frac{n_1}{n_2} = \frac{I_1}{I_2}\frac{\sigma_2}{\sigma_1} \qquad (2)$$

where the peak areas, I_1 and I_2, are corrected for the appropriate cross sections. Other authors have applied this approach to analyzing zeolites (*12, 13*).

Pretreatment of the zeolite in the form of a wafer was carried out in a simple fuzed quartz cell with inlet and outlet stopcocks and a thermocouple well. The cell could be attached either to a manifold for introducing flowing gases or to a vacuum line. Desired temperatures were obtained by heating the sample from room temperature in increments of 100°C/hr up to 400°C. The initial dehydration–deammination step was often followed by reduction in H_2 at 400°C for 16–18 hr. Some reduced samples were further exposed to gases such as air, O_2, or a mixture of H_2 and CO in a 1 : 3 ratio to simulate methanation conditions. The normal flow rate was approximately 30 cm^3/min.

After a complete pretreatment the wafer was cooled in helium to room temperature and the entire cell was evacuated to less than 5×10^{-6} Torr. The cell was opened under a purified N_2 atmosphere in a glove box which was attached to the HP spectrometer. The sample was placed on a gold plate, covered with a retainer window, and inserted into the spectrometer. The time between opening the cell and inserting the mounted wafer into the spectrometer was kept at a minimum to prevent spurious oxidation.

RESULTS

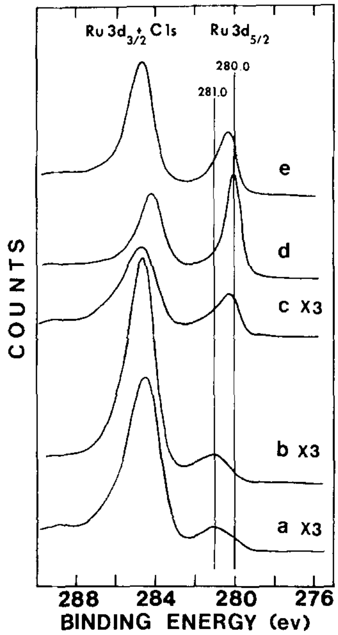

FIG. 1. XPS spectra of Ru $3d_{5/2}$ and Ru $3d_{3/2}$ + C 1s levels of 2% RuNaY (a) degassed in flowing He to 400°C followed by reduction in flowing H_2 for 16–18 hr at 400°C, (b) treated as in (a) with N_2 substituted for He, (c) treated as in (a) followed by heating in flowing CO/H_2 mixture for 24 hr at 280°C and then in H_2 for 18–20 hr at 300°C, (d) treated as in (a) with air substituted for He, and (e) impregnated 1% Ru/NaY treated as in (a).

As depicted in Fig. 1, exposure of the 2% RuNaY zeolite to different gases prior to or following reduction in hydrogen influenced both the intensity and the binding energy of the Ru $3d_{5/2}$ peak. When an inert gas such as He or N_2 was in the dehydration–deammination step, followed by reduction in H_2, nearly identical spectra were obtained (curves a and b). The relatively weak Ru $3d_{5/2}$ peak is characterized by a full width at half maximum (FWHM) of 2.2 eV and a binding energy of 281.0 eV. The Ru $3d_{3/2}$ component should be about 4.1 eV higher in energy (*14*) which would place it on the high energy side of the large C 1s peak. The 0.5% RuNaY sample exhibited a similar spectrum, but with a proportionally lower amplitude ruthenium peak.

The effect of the methanation reaction on the Ru $3d_{5/2}$ peak may be seen in curve c of Fig. 1. After the CO/H_2 mixture flowed over the zeolite for 24 hr at 280°C, the sample was treated for 18–20 hr with pure H_2 at 300°C to remove any carbon overlayer, which may have formed on the ruthenium particles. The ruthenium peak still is characterized by a small amplitude, but the binding energy has decreased to 280.3 eV.

Dehydration in flowing air, followed by reduction in H_2 gave a Ru $3d_{5/2}$ peak (curve d) having about sixfold greater area and a FWHM of 1.0 eV. The binding energy for this peak was at 280.0 eV, which corresponds to the binding energy reported for unsupported Ru^0 (*15*). An X-ray diffraction peak corresponding to $d = 2.056$ of Ru^0 metal was noted for this sample. Applying a simplified Scherrer relation (*16*) to the width of this peak gives a particle size of ca. 250 Å. The peak at 284.1 eV is a combination of the peaks due to C 1s and Ru $3d_{3/2}$. The shift in binding energy of 0.6 eV relative to curves a–c illustrates the errors that one might introduce by using the C 1s peak as a binding energy standard in ruthenium-containing samples.

A similar binding energy for Ru $3d_{5/2}$ was obtained (curve e) for a NaY zeolite impregnated with 1% Ru by weight, after dehydration in He and reduction in H_2. Electron micrographs of this material showed particle sizes 100–300 Å on the surface of the zeolite (*8*).

By using Eq. (2) and the appropriate peak intensities the concentration ratios have been calculated for the zeolite samples. The results are compiled in Table 1 for the samples containing 0.5 and 2.0% Ru by weight. Theoretical ratios for Si/Al, Na/Al, and Ru/Si were calculated from data based on the chemical analysis. Theoretical Ru/Si ratios were based on the assumption that a homogeneous distribution of ruthenium existed inside the zeolite. These theoretical values will be used as the basis for determining whether migration of the ruthenium to the external surface of the zeolite occurred. Although the ratios for Si 2p/Al 2s, Na 2s/Al 2s, and Ru $3d_{5/2}$/Si 2p are given in Table 1, the corresponding Si 2s/Al 2s and Ru $3d_{5/2}$/Si 2s ratios were similar. The Al 2p line was found to be distorted by the Ru 4s

TABLE 1

Concentration Ratios for Ruthenium-Exchanged NaY Zeolite

Wt% Ru	Treatment	Concentration ratios[a]		
		Si 2p/Al 2s	Na 2s/Al 2s	Ru $3d_{5/2}$/Si 2p (× 1000)
0.5	He + H_2, 400°C[b]	2.90	0.84	9
0.5	Air + H_2, 400°C	3.12	0.93	63
Theoretical		2.43	0.95	6
2.0	He + H_2, 400°C	2.95	0.61	19
2.0	He + H_2, 500°C	2.80	0.57	18
2.0	Vac + H_2, 400°C	2.88	0.58	20
2.0	N_2 + H_2, 400°C	3.19	0.57	21
2.0	He + H_2, 400°C; CO/H_2, 280°C; H_2, 300°C	3.04	0.69	22
2.0	Air + H_2, 400°C	3.02	0.64	110
2.0	2.2% O_2/He + H_2, 400°C	2.90	0.62	110
2.0	0.02% O_2/He + H_2, 400°C	3.18	0.62	635
2.0	He + H_2, 400°C; O_2 slow 25°C	2.96	0.52	16
Theoretical		2.43	0.82	24

[a] Area ratios corrected for cross sections, σ: e.g.,

$$\text{Ru } 3d_{5/2}/\text{Si } 2p = \frac{A_{\text{Ru } 3d_{5/2}}}{A_{\text{Si } 2p}} \times \frac{\sigma_{\text{Si } 2p}}{\sigma_{\text{Ru } 3d_{5/2}}} .$$

[b] Indicates that sample was heated to 400°C in flowing He and than reduced in flowing H_2 at 400°C.

line, especially when the Ru on the surface had been enhanced.

The experimental Si 2p/Al 2s ratios are generally larger than the theoretical value of 2.43, but this is consistent with previously reported XPS results for zeolites (*12*, *13*). The Na 2s/Al 2s ratio was independent of pretreatment conditions, although this ratio was about 25% less than the theoretical value for the 2% RuNaY sample. This result suggests that exchange of some sodium ions with protons may have occurred on the external surfaces of the zeolites during the washing step.

The Ru $3d_{5/2}$/Si 2p results show that there is a striking contrast between those samples which were degassed in the presence of oxygen and those that were treated in the absence of oxygen. Less than theoretical Ru $3d_{5/2}$/Si 2p ratios were observed for zeolites reduced in H_2 at either 400 or 500°C, evacuated, and then reduced with H_2 or even exposed to reacting CO/H_2 mixtures for prolonged periods. Oxygen, however, even at levels of 0.02%, brought about Ru $3d_{5/2}$/Si 2p ratios which were from 5 to 30 times the theoretical ratio. At the lower oxygen level the very large ratio is partly a result of a decrease in the area of the Si 2p line. In fact, all of the lines corresponding to Na, Al, Si, and O decreased by approximately a factor of two. This loss in intensity indicates the formation of a dispersed layer of ruthenium on the external surface of the zeolite crystallites.

It was also of interest in this study to determine the state of the ruthenium during dehydration–deammination. In Fig. 2 the photoelectron spectra are shown for samples which were degassed under vacuum or progressively heated to higher temperatures in flowing He. Evacuation at 25°C or heating in He up to 115°C gave poorly resolved ruthenium lines; however, in the latter case a shoulder having a binding energy of ca. 283.0 eV was observed. At 300°C there was a shift to a binding energy of 281.7 eV, and raising the temperature to 400°C caused a further shift to 281.3 eV. As previously noted, the binding energy shifted to 281.0 eV upon reduction in H_2.

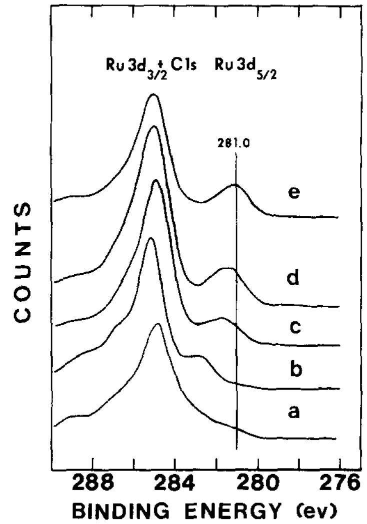

FIG. 2. XPS spectra on Ru $3d_{5/2}$ and Ru $3d_{3/2}$ + C 1s levels of 2% RuNaY (a) after evacuation overnight at 25°C, (b) after degassing in flowing He in increments of 100°C/hr to 115°C, (c) to 300°C, (d) to 400°C, and (e) after treatment as in (d) followed by reduction in flowing H_2 for 16–18 hr at 400°C.

The original ruthenium-ammine zeolites were pink to purple, and it was previously suggested that the purple complex $[Ru^{III}(NH_3)_5(OH)]^{2+}$ was formed by the reaction (*17*)

$$[Ru^{II}(NH_3)_5N_2]^{2+} + H_2O \rightarrow [Ru^{III}(NH_3)_5(OH)]^{2+} + NH_4^+ + N_2. \quad (3)$$

Madhusudhan *et al.* (*18*) have recently presented evidence that the color may be that of ruthenium-red,

$$(NH_3)_5Ru^{III}\text{-}O\text{-}Ru^{IV}(NH_3)_4\text{-}O\text{-}Ru^{III}(NH_3)_5.$$

For our original samples at room temperature the N 1s peak exhibited two components: a strong peak at 400.9 eV which corresponds to coordinated NH_3 and a weak shoulder at approximately 403 eV which corresponds to the binding energy of nitrogen in NH_4Y zeolites. The labile NH_3 in Eq. (3) may be the source of the NH_4^+ intensity. Both peaks decreased in area upon heating the sample to 112°C. This decrease in area together with the shift in binding energy of the ruthenium is consistent with the previous results which suggested that the coordinated ammonia partially reduced the ruthenium.

Since the presence of O_2 caused significant changes in binding energies and Ru $3d_{5/2}$/Si 2p ratios, two studies were carried out to determine the conditions under which oxygen had an effect on the state of the ruthenium. In the first case the sample was exposed to air at progressively higher temperatures, and the resulting spectra are shown in Fig. 3. Up to 200°C the spectrum (curve a) resembles that of the sample evacuated at room temperature (Fig. 2, curve a). Exposure of the sample to oxygen at 300 or 400°C (curve b) resulted in an increase in the Ru $3d_{5/2}$ peak area by a factor of 5 and a shift in binding energy to 281.0, which agrees with the value of 280.7 for RuO_2 as reported by Kim and Winograd (*15*). Mössbauer data also indicate that oxidation of a RuY zeolite at 400°C in air yielded RuO_2 (*19*). A final reduction in H_2 caused the expected shift in binding energy to 280.1 eV with no additional change in peak area.

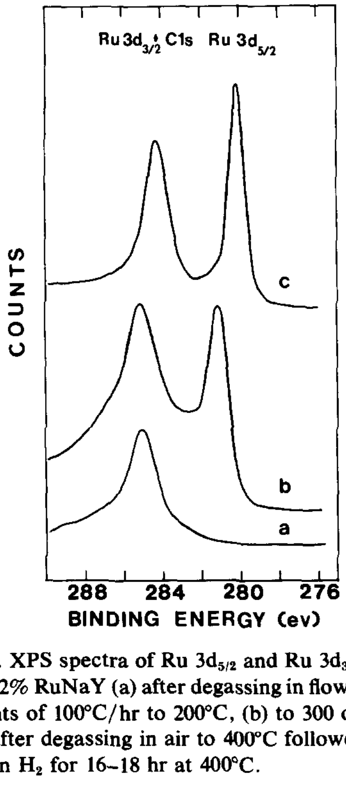

FIG. 3. XPS spectra of Ru $3d_{5/2}$ and Ru $3d_{3/2}$ + C 1s levels of 2% RuNaY (a) after degassing in flowing air in increments of 100°C/hr to 200°C, (b) to 300 or 400°C, and (c) after degassing in air to 400°C followed by reduction in H_2 for 16–18 hr at 400°C.

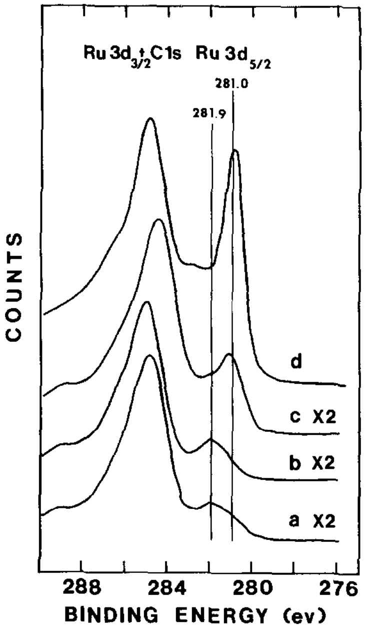

FIG. 4. XPS spectra of Ru $3d_{5/2}$ and Ru $3d_{3/2}$ + C 1s levels of reduced 2% RuNaY after exposure to (a) a slow addition of O_2 to 300 Torr over a period of 2 hr at 25°C, (b) ambient atmosphere for 30 days, (c) flowing dry air for 1 hr at 25°C, and (d) flowing O_2 for 2 hr at 400°C.

In the second oxygen study a zeolite which had only been heated in He and reduced in H_2 was exposed to oxygen under various conditions. These experiments were carried out to determine the susceptibility of the ruthenium to oxidation, and in particular the extent to which ruthenium might be oxidized by O_2 impurities in the glove box. Introduction of O_2 up to 300 Torr via a slow leak, with the sample at 25°C, resulted in the spectrum shown in curve a of Fig. 4. The small Ru $3d_{5/2}$ peak had a binding energy of 281.9 eV. A similar spectrum (curve b) was observed after the reduced sample had been left in the ambient atmosphere for 30 days. An increase in area and shift in binding energy to 281.0 eV was observed (curve c) when the sample was immediately exposed to 152 Torr of O_2 in dry air which was flowed over the zeolite wafer. Lastly, heating the sample in O_2 at 400°C resulted in the spectrum of curve d, which resembles that spectrum observed after treating the original unreduced sample in dry air to 400°C (Fig. 3, curve b).

Binding energies, together with assignments of the oxidation state and location of ruthenium in the zeolite, are summarized in Table 2.

DISCUSSION

Based on the concentration ratios listed in Table 1 we conclude that reduced ruthenium particles remain within the zeolite cavities provided oxygen is excluded from the system. Additional evidence for Ru^0 may be found in the Mössbauer studies of Clausen and Good, who observed that the reduction of RuY zeolites by H_2 at 400°C resulted in metal particles <80 Å in diameter (*19*). Even after the methanation reaction, in which H_2O was produced as a by-product, the ruthenium remained within the zeolite; however, a decrease in binding energy from 281.0 to 280.1 eV indicates that a modification has occurred in the state of the ruthenium. This modification coincides with a particle growth from < 10 Å to ca. 15 Å as previously reported (*1*).

Although it is tempting to attribute the binding energy shift of 0.9 eV to a metal–support interaction, there are several factors which may contribute to the effect. A similar shift in binding energy was noted by Kim and Winograd (*20*) for Au atoms which had been implanted in SiO_2, relative to Au supported on the surface. They interpreted the binding energy difference, ΔBE, in terms of the equation

$$\Delta BE = (\Delta q/r) - (\Delta V + \Delta E_R + \Delta Q) \quad (4)$$

where $\Delta q/r$ is the chemical shift resulting from a change in the valence electron charge on the implanted atom and ΔV, ΔE_R, and ΔQ are the differences in the crystal field potential energy, the relaxation energy, and the work function, respectively. The latter three terms have been viewed as the matrix effect of the SiO_2; however, when applied to our study they would also include the effect of the neighboring ruthenium atoms. Although it is not possible at this time to determine the magnitude of each term, it is clear that such factors as the change in band structure with the increase in particle size and possible electron transfer from the cluster to the zeolite may affect the binding energy of the ruthenium. The results suggest, however, that once that particle has reached a diameter of about 15 Å, further increase in size does not alter the binding energy, even though the particle may migrate to the external surface of the zeolite.

TABLE 2

Descriptions of the State of Ru in Pretreated RuNaY

Sample treatment	BE (eV) Ru $3d_{5/2}$	Description
Vac, 25°C	~283.0	Ru^{III} ammine; internal
He, 115°C	282.9	Ru^{III} Gradual change with over-
300°C	281.7	↓ lapping of oxidation
400°C	281.4	Ru^{I} states; all internal
He + H_2, 400°C	281.0	Ru^0 <10 Å diameter; internal
He + H_2, 400°C; CO/H_2, 280°C; H_2, 300°C	280.1	Ru^0 ca. 15 Å diameter; internal
O_2 + H_2, 400°C	280.0	Ru^0 ca. 250 Å diameter; external
O_2, 300°C or 400°C	281.0	RuO_2 external
He + H_2, 400°C; O_2, slow, 25°C	281.9	RuO_2 internal

Similar conclusions may be reached concerning the oxidized form of ruthenium, which is presumably RuO_2. The data of Fig. 4 suggest that the ruthenium clusters may be oxidized at 25°C, and that they will remain within the zeolite provided the oxygen is added slowly in order to prevent a thermal excursion. Oxidation at elevated temperatures results in the migration of the particles to the external surface, which is accompanied by a decrease in binding energy of 0.9 eV. Thus it appears that a similar mechanism is responsible for the larger binding energies, both for the Ru^0 and the RuO_2 clusters within the zeolite. It is interesting to observe that the common factor between the two systems is the zeolite matrix.

Ruthenium ions may also be oxidized to RuO_2 on the external surface of the zeolite. This raises a question concerning charge compensation within the zeolite, i.e., what cation replaces the ruthenium? The mechanism may be similar to that found in the dehydroxylation reaction where charge balance is accomplished by the removal of an oxygen from the lattice as water. In a similar manner one of the oxygens in RuO_2 may be derived from the lattice. This type of phenomenon also occurs in zeolites when metal ions such as Cu^{2+} are reduced by CO with the production of CO_2 (*21*). Once formed the RuO_2 must be able to migrate to the external surface.

The state of ruthenium in the zeolite prior to reduction or oxidation is more difficult to establish from the XPS data. Since the Ru 3d lines strongly overlap the C 1s line, it was not possible to determine binding energies for the ruthenium ammine complex accurately. Mixtures of $[Ru(NH_3)_6]^{3+}$ and NaY zeolite exhibited Ru $3d_{5/2}$ and Ru $3d_{3/2}$ binding energies of 282.9 and 286.9 eV, respectively. Mössbauer experiments on the pink form of the zeolite indicate that the metal is present as Ru^{III} (*19*). As the temperature is raised to 300°C there is a reduction of Ru^{III} to a lower oxidation state which is currently thought to be Ru^{I}. Repeated experiments confirm that the binding energy of this species is distinctly different from that of Ru^0, as shown in curves d and e of Fig. 2.

CONCLUSIONS

It is possible to form ruthenium metal particles within the zeolite cavities provided O_2 is excluded from the system. In the presence of oxygen at elevated temperatures, either before or after reduction, RuO_2 is formed on the external surface of the zeolite. This is in contrast to the results reported for Pt in zeolites, where oxygen stabilized the metal within the zeolite (*22*).

Reduction of the ruthenium results in clusters which show a significant increase in binding energy relative to larger particles located either in the large cavities or on the external surface of the zeolite. Assignment of this phenomenon specifically to partial oxidation of the metal or to matrix effects cannot be made at this time. The results point out, however, that care must be exercised when comparing binding energies for molecules within zeolites to those of known compounds outside the zeolite environment.

ACKNOWLEDGMENTS

The authors wish to acknowledge the support of this work by the Division of Basic Energy Sciences, Department of Energy, and the Center for Energy and Mineral Resources, Texas A&M University. Preliminary experiments were carried out by Drs. M. J. Lin and W. DeWilde and by Mr. J. R. Pearce.

REFERENCES

1. Elliott, D. J., and Lunsford, J. H., *J. Catal.*, **57**, 11 (1979).

2. Dalla Betta, R. A., Pilsen, A. G., and Shelef, M., *J. Catal.* **35**, 54 (1974).

3. Minachev, Kh. M., Antoshin, G. V. Shpiro, E. S., and Navruzov, T. A., *Izv. Akad. Nauk SSR, Ser. Khim.* 2131 (1973).

4. Minachev, Kh. M., Antoshin, G. V. Shpiro, E. S., and Isakov, Ya. I., *Izv. Akad. Nauk SSR, Ser. Khim.* 2134 (1973).

5. Herman, R. G., Lunsford, J. H., Beyer, H., Jacobs, P. A., and Uytterhoeven, J. B., *J. Phys. Chem.* **79**, 2388 (1975).

6. Kobylinski, T. P., Taylor, B. W., and Young, J. E., *Trans. Soc. Auto. Eng.* **83**, 1089 (1974).

7. Fiedorow, R. M. J., Chahar, B. S., and Wanke, S. E., *J. Catal.* **51**, 193 (1978).

8. Rommanikov, V. N., Pedersen, L. A., and Ione, K. G., to be published.

9. Defosse, C., Friedman, R. M., and Fripiat, J., *Bull. Chim. Soc. Fr.* 1513 (1975).

10. Scofield, J. H., *J. Electron Spectrosc.* **8**, 129 (1976).

11. Wagner, C. D., *Anal. Chem.* **49**, 1282 (1977).

12. Tempere, J. Fr., Delafosse, D., and Contour, J. P., "Molecular Sieves-II" (J. R. Katzer, Ed.), p. 76. The American Chemical Society, 1977.

13. Defosse, C., Delmon, B., Canesson, P., "Molecular Sieves-II" (J. R. Katzer, Ed.), p. 86. The American Chemical Society, 1977.

14. Citrin, P. H., *J. Amer. Chem. Soc.* **95,** 6472 (1973).

15. Kim, K. S., and Winograd, N., *J. Catal.* **35,** 66 (1974).

16. Innes, W. B., *in* "Experimental Methods in Catalytic Research" (R. B. Anderson, Ed.), Vol. 1, p. 84. Academic Press, New York, London, 1968.

17. Laing, K. R., Leubner, R. L., and Lunsford, J. H., *Inorg. Chem.* **14,** 1400 (1975).

18. Madhusudhan, C. P., Patil, M. D., and Good, M. L., *Inorg. Chem.* **18,** 2384 (1979).

19. Clausen, C. A., and Good, M. L., *Inorg. Chem.* **16,** 816 (1977).

20. Kim, K. S., and Winograd, N., *Chem. Phys. Lett.* **30,** 91 (1975).

21. Naccache, C. M., and Ben Taarit, Y., *J. Catal.* **22,** 171 (1971).

22. Gallezot, P., Alarcon-Diaz, A., Dalmon, J-A., Renouprez, A. J., and Imelik, B., *J. Catal.* **39,** 334 (1975).